

# Ionic Clustering in Amine-Capped Telechelic Ionomers from ESR of Cupric Complexes

Hongqing Xue<sup>†</sup> and Shulamith Schlick\*

Department of Chemistry, University of Detroit Mercy, Detroit, Michigan 48219-3599

Received December 26, 1991; Revised Manuscript Received May 5, 1992

**ABSTRACT:** ESR spectra of  $\text{Cu}^{2+}$  complexes in amine-terminated telechelic polybutadiene were measured, in order to obtain local information on the bonding in the cupric site. The increase in the line widths with cation content indicates the process of cation clustering. The intercation distances deduced from the broadening of the ESR lines are much shorter than those calculated by assuming of a homogeneous cation distribution and approach the Cu-Cu distance in  $\text{CuCl}_2 \cdot 2\text{H}_2\text{O}$ . Diamagnetic dilution by  $\text{Zn}^{2+}$  allows observation of the details of polymer complexation with high resolution, even at a combined ( $\text{Cu}^{2+}$  and  $\text{Zn}^{2+}$ ) cation content 6 times higher than the theoretical amount needed for full complexation. The results obtained in this study indicate that the cation site is very sensitive to the total cation content. At a low degree of complexation  $\text{Cu}^{2+}$  is connected to the polymer through four  $^{14}\text{N}$  ligands. The number of nitrogen ligands decreases as the amount of cation increases. For a combined cation content 3 times higher than that needed for full complexation, the cations appear to form ionic domains *isolated* from and *unconnected* to the polymer chains. The results obtained describe the complexity of the polymer bonding to the cation and indicate explicitly the various cation sites. The break in the polymer bonding to the cation at high cation content and the existence of the isolated ionic domains explain two effects discussed in the literature, the fact that both the  $T_g$  and the chain dimensions are *not* affected by the presence of the cations.

## Introduction

Amphiphilic polymers such as ionomers have a complex morphology, which is frequently described in terms of phase separation between organic and polar domains.<sup>1</sup> Important parameters that describe the polymer morphology are the domain size and the extent of phase separation; these parameters are measured as a function of chain length, the nature and concentration of the ionic groups, temperature, and swelling solvent. Small-angle X-ray and neutron scattering, SAXS and SANS, respectively, have been used extensively to prove the existence of the separated structure and to determine an *average* size of the ionic clusters.<sup>1-3</sup> Spectroscopic methods have provided *local* structural information on the formation of hydrogen bonds, on chain dynamics, and on the immediate neighbors and symmetry of the ionic sites.<sup>4-8</sup>

Each of the main methods of study has serious limitations. Scattering experiments provide data that are used to verify proposed theoretical models; while the calculations include a large number of parameters, the number of experimental features is small. Spectroscopic methods probe a limited space around the reporter molecule or ion and are sometimes considered to be of limited use for understanding the macroscopic properties of the system. Some recent results have stressed the importance of considering the information obtained from *both* methods of study in describing the ionomer morphology. In the case of perfluorinated ionomer membranes the ionic peaks measured in SAXS experiments are similar for the membranes swollen by water and methanol;<sup>9</sup>  $^{19}\text{F}$  NMR data, however, strongly suggest a complete phase separation for water as solvent but significant penetration of methanol and other alcohols into the organic domains.<sup>10</sup>

Telechelic ionomers, which consist of polymer chains terminated on both ends by ionic groups, have been considered as model compounds because of their simple structure, compared with ionomers containing ionic groups on randomly distributed pendant chains.<sup>11</sup> Extensive

studies have been reported on dicarboxylic telechelic polybutadiene (CTPB) and polyisoprene (CTPI), on disulfonated telechelic polystyrene (STPS), and also on cationic ionomers.<sup>12-17</sup> The slow rate of water uptake in CTPB ionomers has been interpreted as an indication for the existence of *isolated* ionic domains.

SAXS measurements on CTPB and CTPI have been performed as a function of temperature, degree of neutralization, swelling by different solvents, and chain length. The results indicate that the average size of the ionic domains is independent of the type of cation used to neutralize the acid ionomer, in contrast to the rheological properties of the ionomers, which are very sensitive to the nature of the cation. This discrepancy has been related to the assumption of a spherical domain shape in the analysis of SAXS results or to the existence of a nonuniform spatial distribution of the ionic domains.<sup>12</sup> The glass transition temperatures  $T_g$  measured by differential scanning calorimetry (DSC) appear to be insensitive to the presence of ions. Studies of the proton relaxation times  $T_1$ ,  $T_2$ , and  $T_{1\rho}$  by NMR in these systems have suggested the possibility that the effect of the ions on the  $T_g$  values is not observed because the amount of material in the vicinity of the ions is small,  $\leq 10\%$ , and is not reflected in the *average*  $T_g$  values detected by DSC.<sup>18</sup>

Similar observations have been reported for amino-terminated polydienes complexed with  $\text{CuCl}_2$  and  $\text{FeCl}_3$  studied by SAXS, DSC, and dynamic mechanical relaxation.<sup>14</sup>

In this report we present results obtained in a study of amine-terminated polybutadiene (ATPB) complexed by  $\text{Cu}^{2+}$ , using electron spin resonance (ESR). This study was motivated by our interest to correlate the macroscopic properties of the ionomer with the local environment of the cation as a function of cation content and temperature. The method of diamagnetic dilution of  $\text{Cu}^{2+}$  by  $\text{Zn}^{2+}$  allows observation of well-resolved ESR spectra from the paramagnetic cation in the presence of a large total amount of complexing cations.

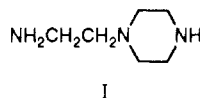
The telechelic ionomers are different in many aspects from the perfluorinated ionomers containing pendant chains terminated by sulfonic acid groups (PFSA) that we

<sup>†</sup> On leave from the Shanghai Institute of Testing Technology, 716 Yi Shan Road, Shanghai, People's Republic of China.

have studied recently.<sup>8,9,19-23</sup> The perfluorinated ionomers are very hygroscopic, and samples must be carefully prepared in a dry atmosphere in order to obtain reproducible results.<sup>24</sup> In the telechelic ionomers the ionic domains appear to be isolated, and the diffusion of polar solvents is considerably slower; this property simplifies the procedure of sample preparation. The PFSA ionomers such as Nafion are available as membranes which are permselective for cations.<sup>2</sup> In most cases the maximum degree of neutralization is  $\leq 90\%$ ; in the telechelic ionomers higher cation contents can be obtained, because the complexing cation in the form of salt is mixed with the liquid polymer. In this way it is possible to incorporate cation amounts that are several times larger than those necessary for full complexation of the end groups. The structural simplicity of the telechelic ionomers is an important advantage.

## Experimental Section

**Preparation of ATPB.** The  $\alpha,\omega$ -dicarboxylic polybutadiene (CTPB), tradename Hycar CTB 2000  $\times$  162 ( $M_n = 4200$ , functionality = 1.9, and specific gravity at 25 °C = 0.907), was supplied by B.F. Goodrich. The diamine-terminated ionomer (ATPB) was prepared by reaction with the amine 1-(2-aminoethyl)piperazine from Aldrich (AEP, I) according to published



methods.<sup>25</sup> The percentage of unreacted acid groups was determined by dissolving ATPB in a mixture of toluene and 2-propanol (60:40 by volume) and titration with a standard KOH solution. We deduced that only 3.8% of the initial acid groups remained unreacted with the amine; this value is within normal limits for the reaction.<sup>25</sup>

**Complexation with  $\text{Cu}^{2+}$ .** A solution of  $\text{CuCl}_2 \cdot 2\text{H}_2\text{O}$  in methanol, containing also  $\text{ZnCl}_2$  in the case of diamagnetic dilution, was added dropwise ( $\approx 5$  mL/h) with stirring to 100 mL of a polymer solution in toluene (3–5% by weight) at ambient temperature under nitrogen. In order to maintain a constant volume ratio of the chloride solution to the polymer solution ( $\approx 7/100$ ), the concentration of the chloride in methanol varied, depending on the  $\text{Cu}^{2+}$ /amine and  $\text{Zn}^{2+}$ /amine molar ratio,  $x(\text{Cu})$  and  $x(\text{Zn})$ , respectively. The total cation/amine molar ratio is  $x(\text{total})$ . For  $x(\text{Cu}) \leq 1.0$  no precipitation occurred and the solution was homogeneous during the complexation process. For  $x > 1.0$  a red-brown precipitate was formed. For complexation of the ionomer with a mixture of  $\text{Cu}^{2+}$  and  $\text{Zn}^{2+}$  ions, the precipitation appears to depend only on the amount of  $\text{Cu}^{2+}$ . The color of the complex solution changed gradually from green to green-yellow, to brown, and to red-brown as  $x(\text{Cu})$  increased from 0.02 to 3.0.

The polymer complexes were separated from the solvents by distillation in vacuo at ambient temperature, dried in vacuo for 3 days, washed three times with methanol, and finally dried as before to constant weight.

**ESR Spectra.** Spectra at X-band were measured with a Bruker 200D SRC spectrometer operating at 9.7 GHz (empty cavity at ambient temperature) and 100-kHz magnetic field modulation, interfaced with a data acquisition system based on an IBM PC/XT and the software EPRDAS (Mega Systems Solutions, Rochester, NY). Samples were cooled using the Bruker flow system 4111VT. The microwave frequency was measured with the HP 5342A frequency counter. Calibration of  $g$  values is based on a  $\text{Cr}^{3+}$  in MgO standard ( $g = 1.9796$ ). All spectra were recorded at a microwave power of 2 mW except when otherwise indicated.

Spectra were simulated by an HP Vectra RS/20C computer, using Pascal 5.0 codes developed in our laboratory.<sup>22</sup> For ease of comparison, all experimental and simulated spectra were transformed into the format used by EPRDAS, using a Pascal program.

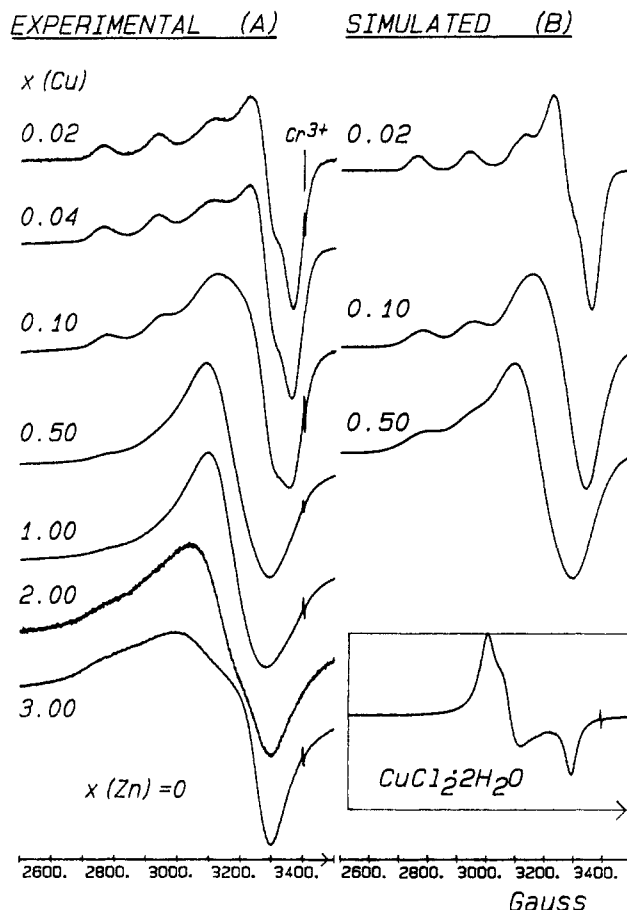


**Figure 1.** (A) X-band ESR spectra at 125 K of  $\text{Cu}^{2+}$  in ATPB for  $x(\text{Zn}) = 0$  and the indicated values of  $x(\text{Cu})$ . The inset is the X-band ESR spectrum of  $\text{CuCl}_2 \cdot 2\text{H}_2\text{O}$  powder at 125 K, on a scan of 1000 G. (B) Simulated spectra for the indicated values of  $x(\text{Cu})$ , using the parameters given in Table I.

## Results

**1. ESR Spectra.** ESR spectra will be described as a function of cation content expressed as  $x(\text{Cu})$ ,  $x(\text{Zn})$ , and  $x(\text{total})$ . We note that for  $x(\text{total}) = 0.5$  all amine groups are theoretically complexed by the metal cations.

In Figure 1A we present X-band ESR spectra of the copper complexes of ATPB at 125 K and  $x(\text{Zn}) = 0$ , as a function of  $x(\text{Cu})$ . For the lowest  $\text{Cu}^{2+}$  content,  $x(\text{Cu}) = 0.02$ , the ESR parameters obtained by simulation (vide infra) are as follows.  $g_{\parallel} = 2.2240$ ,  $g_{\perp} = 2.0563$ ,  $A_{\parallel} = 0.0187$   $\text{cm}^{-1}$ ,  $A_{\perp} = 0.0013$   $\text{cm}^{-1}$  (site 1). These parameters are typical for a copper complex with four  $^{14}\text{N}$  ligands in the equatorial plane.<sup>26</sup> The large widths of the parallel signals are additional evidence for unresolved  $^{14}\text{N}$  superhyperfine splittings (shf).<sup>21,22</sup> Replacement of the  $\text{CuCl}_2$  enriched in  $^{63}\text{Cu}$  did not change the line shape, an indication that the line width is dominated by magnetic interactions with the ligands and not by the presence of a  $^{63}\text{Cu}$  and  $^{65}\text{Cu}$  isotope mixture. Because of this result, we continued the entire study with the isotopically normal salt.

For  $x(\text{Cu}) > 0.10$  the line widths increase gradually, a phenomenon we assign to magnetic dipolar interactions between cupric ions. For  $x(\text{Cu}) > 1$  the line shapes change, and the ESR spectrum approaches that observed for the pure  $\text{CuCl}_2 \cdot 2\text{H}_2\text{O}$  powder at 125 K shown in the inset;<sup>27</sup> these changes indicate increasing clustering and loss of hyperfine structure due to the onset of exchange interactions.

In contrast to the situation in carboxyl-terminated polybutadiene (CTPB),<sup>5</sup> no ESR signals from cupric dimers have been detected, neither in the  $g = 2$  magnetic field

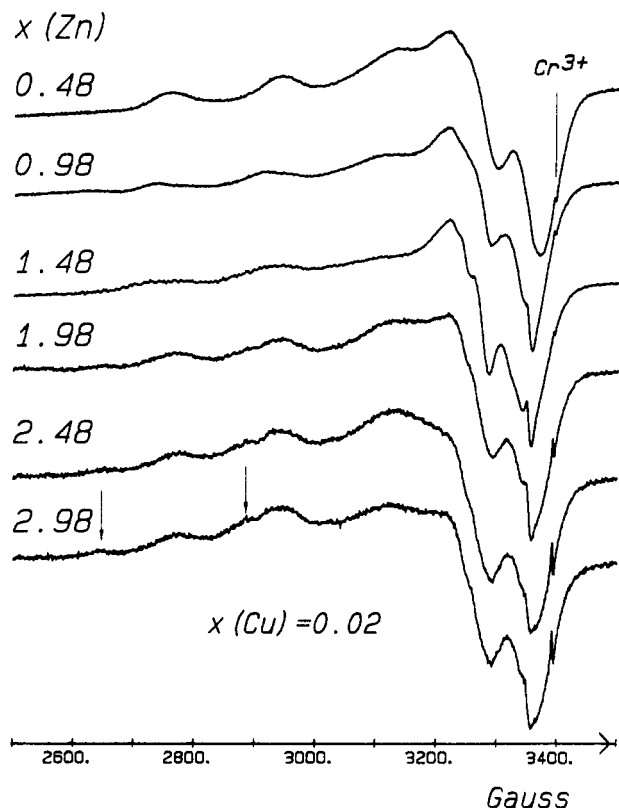


**Figure 2.** X-band ESR spectra at 125 K of  $\text{Cu}^{2+}$  in ATPB for  $x(\text{Cu}) = 0.02$  and the indicated values of  $x(\text{Zn})$ . Downward arrows indicate the positions of the additional *parallel* signals, at high  $\text{Zn}^{2+}$  content.

region for the  $\Delta m_s = 1$  transition nor in the half-field region around 1500 G for the  $\Delta m_s = 2$  transition.

The effect of diamagnetic dilution by  $\text{Zn}^{2+}$  is shown in Figure 2 for  $x(\text{Cu}) = 0.02$  and in Figure 3 for  $x(\text{Cu}) = 0.50$ , as a function of  $x(\text{Zn})$ . The maximum total cation content is 3.0 in both sets of spectra.

For  $x(\text{Cu}) = 0.02$  and  $x(\text{Zn}) = 0.48$  in Figure 2 the parameters for the cupric site, determined by simulation, are  $g_{\parallel} = 2.2240$ ,  $g_{\perp} = 2.0480$ ,  $A_{\parallel} = 0.0187 \text{ cm}^{-1}$ , and  $A_{\perp} = 0.0019 \text{ cm}^{-1}$  (site 2). Ligation with four  $^{14}\text{N}$  ligands seems to be maintained for this  $\text{Zn}^{2+}$  content. Comparison with the parameters deduced for site 1 indicates that the presence of  $\text{Zn}^{2+}$  leads to a slight change in the local structure, most likely in the *axial* position only,<sup>28</sup> because the  $g_{\parallel}$  values are identical. It is possible that chlorine ligands in the axial positions are responsible for the slight variation in  $g_{\perp}$ . For  $x(\text{total}) \geq 1.0$  the line widths in the parallel region increase significantly; for  $x(\text{total}) \geq 2.0$  additional signals appear and are indicated by the downward arrows. The presence of the signals at lower magnetic fields suggests a larger  $g$  value and therefore a smaller degree of complexation to nitrogen ligands.<sup>26</sup>

For  $x(\text{Cu}) = x(\text{Zn}) = 0.5$  in Figure 3 the components of the parallel signal are spread over a large magnetic curve field, indicating multiple sites for  $\text{Cu}^{2+}$ . The upward arrows correspond to the parallel signals respectively for site 1, indicating the presence of a cupric site with four  $^{14}\text{N}$  ligands, in addition to the other sites. Significant changes in the spectra appear for  $x(\text{Cu}) = 0.5$  and  $x(\text{Zn}) = 1.0$ : the dominant parallel signals, shown more clearly in the vertically expanded spectra and the corresponding "stick" diagrams, are assigned to the additional sites 3 and 4. The following parameters were deduced directly from the spectra.

For site 3,  $g_{\parallel} = 2.3111$  and  $A_{\parallel} = 0.01699 \text{ cm}^{-1}$ .

For site 4,  $g_{\parallel} = 2.2909$  and  $A_{\parallel} = 0.01726 \text{ cm}^{-1}$ .

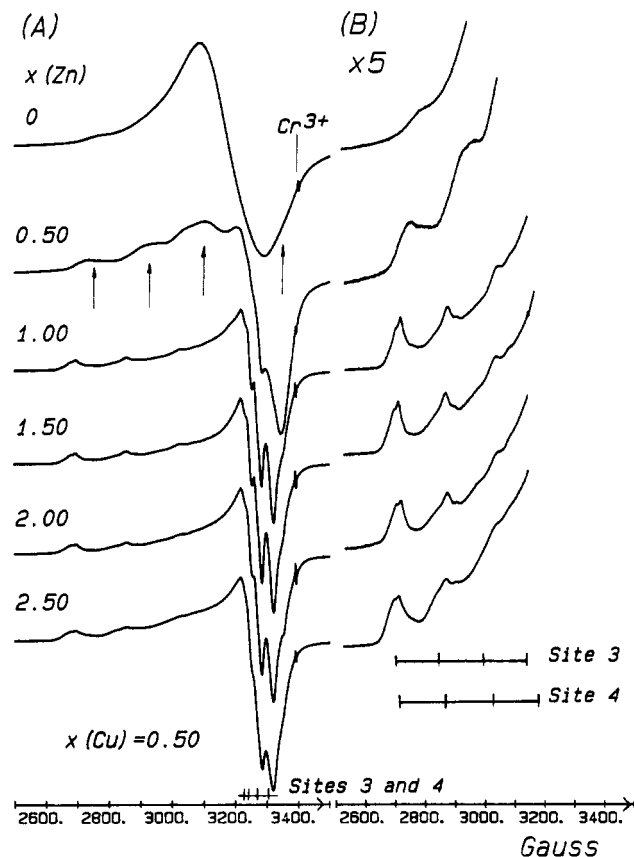


**Figure 3.** X-band ESR spectra at 125 K of  $\text{Cu}^{2+}$  in ATPB for  $x(\text{Cu}) = 0.50$  and the indicated values of  $x(\text{Zn})$ . Full spectra are shown in A and vertically expanded spectra ( $\times 5$ ) in B. Upward arrows correspond to the parallel signals for site 1. "Stick" diagrams indicate the parallel signals for sites 3 and 4 in the expanded spectra (B) and the corresponding perpendicular quartet in the full spectra (A).

For both sites  $g_{\perp} = 2.0626$ . The well-resolved perpendicular quartet, also indicated in Figure 3 by the "stick" diagram, is assigned to Cu hyperfine, giving  $A_{\perp} = 0.0026 \text{ cm}^{-1}$ . The unequal spacing of the perpendicular signals is due to second-order corrections and is expected to be more pronounced for the *smaller* hyperfine tensor component.<sup>28</sup>

The higher  $g_{\parallel}$  and lower  $A_{\parallel}$  values indicate that the number of  $^{14}\text{N}$  ligands is less than four.<sup>26</sup> Because the  $^{14}\text{N}$  shf splitting is  $\approx 15 \text{ G}$ , the resolution in the perpendicular region appears possible only if the nitrogen ligation is absent. It seems that for  $x(\text{Cu}) = 0.50$  and  $x(\text{Zn}) \geq 1.0$  no evidence for  $^{14}\text{N}$  ligation is found. The narrower widths of the parallel signals, seen more clearly in the vertically expanded spectra, provide additional support for this conclusion.

**2. Simulations.** ESR spectra for  $x(\text{Zn}) = 0$  as a function of  $x(\text{Cu})$  were simulated in an attempt to follow the process of cation clustering. In calculating the spectra we assumed axial  $g$ , hyperfine and superhyperfine tensors, with a common principal axes system. Line positions were calculated to second order for Cu hyperfine and to first order for superhyperfine signals, and all  $^{14}\text{N}$  ligands were considered identically bonded. The line shapes were a combination of Gaussian and Lorentzian components, chosen to obtain the best visual fit. Additional computational details have been reported.<sup>22</sup> The main objective of the simulations was to determine the line widths  $\Delta H$  (full width at half-maximum intensity) as a function of  $x(\text{Cu})$  and to calculate the *increase* in the line width  $\delta(\Delta H)$  compared to the line width for the lowest value of

Table I  
ESR Parameters and Interaction Distances<sup>a,b</sup>

X(Cu)	$g_{\parallel}$	$g_{\perp}$	$A_{\parallel}$ (cm <sup>-1</sup> )	$A_{\perp}$ (cm <sup>-1</sup> )	$\Delta H_{\parallel}$ (G)	$\Delta H_{\perp}$ (G)	$d$ (ESR) (Å)	$d$ (hom) (Å)
0.02	2.2240	2.0563	0.0187	0.0013	17	30		63
0.10	2.2240	2.0700	0.0178	0.0019	90	110	7.9 (9.5) <sup>c</sup>	37
0.50	2.2240	2.1100	0.0171	0.0020	140	150	6.7 (8.0) <sup>c</sup>	22

<sup>a</sup> All spectra were simulated for the strain parameters  $\delta g = 0.0250$ ,  $\delta A = 16$  G. Four <sup>14</sup>N ligands were considered, with  $A_{\parallel}(\text{shf}) = 15$  G and  $A_{\perp}(\text{shf}) = 14$  G.<sup>22</sup> <sup>b</sup> The line shapes were a mixture of Gaussian and Lorentzian components, with identical weights. <sup>c</sup> Values in parentheses are for a cubic lattice and also for hexagonal arrays of cations.

$x(\text{Cu})$ . This increase is assigned to magnetic dipole–dipole interactions.<sup>19</sup>

Simulated spectra for  $x(\text{Cu}) = 0.02$ , 0.10, and 0.50 are given in Figure 1B, based on the parameters given in Table I. The “strain” parameters  $\delta g$  and  $\delta A$  were similar to those used in our previous publications.<sup>19,20,22</sup> The effect of these parameters was important only to simulate the ESR spectrum for  $x(\text{Cu}) = 0.02$ ; in the other cases, the line widths were the dominant factor. In all simulations given in Figure 1B we assumed *four* <sup>14</sup>N ligands. The spectrum corresponding to  $x(\text{Cu}) = 0.10$  was well reproduced also by assuming *two* nitrogen ligands only; in the case of  $x(\text{Cu}) = 0.50$  the line widths used to simulate the experimental results were so large that the number of nitrogen ligands had no effect on the calculated line shapes. Although the number of parameters needed to simulate the ESR spectra is large, their effect is specific and can be chosen with reasonable confidence. Therefore, the agreement between the simulated and the corresponding experimental spectra is considered satisfactory.

The increase in the line width  $\delta(\Delta H)$  is similar for the parallel and perpendicular components; for simplicity we will only consider the values for the parallel components.<sup>19</sup>

The distance  $d$  between interaction magnetic dipoles can be calculated by observing that for a linear array of dipoles the dipolar contribution to the line width,  $\delta(\Delta H)$ , is given by eq 1,<sup>29</sup> where  $\beta_e$  is the Bohr magneton.

$$\delta(\Delta H) = 2[(6/5)g^2\beta_e^2S(S+1)]^{1/2}d^{-3} \quad (1)$$

The relation between the intercation distance  $d$  (in angstroms) and the observed dipolar contribution  $\delta(\Delta H)$  (in gauss) can be written as in eq 2. The isotropic value of  $g$  can be used to deduce  $d$ .

$$\delta(\Delta H) = 5672.4g^2d^{-3} \quad (2)$$

For a cubic lattice or a hexagonal array of cations the numerical term in eq 2 should be multiplied by  $\sqrt{3}$ .

The values of  $d$  for  $x(\text{Cu}) = 0.10$  and 0.50 calculated from the simulations of experimental spectra are given in Table I for the two models. The values in parentheses are for a cubic lattice.

## Discussion

In this section we will discuss cation clustering in ATPB containing cupric ions (no zinc) and the changes in the bonding of the cations to the polymer in the presence of a large total cation content ( $\text{Cu}^{2+}$  and  $\text{Zn}^{2+}$ ).

The intercation distances, assuming a homogeneous distribution of cations, can be calculated from the ionomer composition and density. The values obtained for a simple cubic lattice are given in Table I for  $x(\text{Cu}) = 0.02$ , 0.10, and 0.50. It is immediately clear that the distances calculated from the line widths of ESR spectra are significantly smaller, indicating clustering of the cations even when  $x(\text{Cu}) = 0.10$ , much less than the total amount needed to complex all terminal amine groups. For com-

plexation of *all* amine groups ( $x(\text{Cu}) = 0.50$ ) the intercation distance is 6.7 Å if a linear array of cations is assumed. It is expected that in the samples containing higher amounts of  $\text{Cu}^{2+}$  the distance is even shorter and approaches the value of 5.457 Å in  $\text{CuCl}_2 \cdot 2\text{H}_2\text{O}$ ; the intercation distance is shorter in anhydrous  $\text{CuCl}_2$ , 3.802 Å.<sup>30</sup> The changes in the ESR spectra in Figure 1A for  $x(\text{Cu}) \geq 2.0$  indicate this trend.

The slight changes in the parameters used for the simulation of ESR spectra indicate a change in the immediate surroundings of the cation as a function of cation content. The changes cannot be detected very accurately in samples containing a high content of  $\text{Cu}^{2+}$ , because of the broad lines. These changes in the ESR spectra can be detected with greater resolution in samples containing  $\text{Zn}^{2+}$  as the diamagnetic diluent. ESR spectra presented in Figures 2 and 3 indicate that the local environment of the cupric ions is very sensitive to the cation content and point to a *break* of the cation bond to the polymer as the amount of cations increases. Even for a very low copper content ( $x(\text{Cu}) = 0.02$ ), addition of  $\text{Zn}^{2+}$  results in a distribution of sites for the paramagnetic cation and indicates that less than 4% of the total amount of cupric ions are ligated to the polymer through four <sup>14</sup>N ligands when  $x(\text{Zn}) \geq 1.0$ . The remaining  $\text{Cu}^{2+}$  cations have a smaller number of ligands from the polymer.

The effect of added  $\text{Zn}^{2+}$  is clearly visible in Figure 3, for a fixed copper content,  $x(\text{Cu}) = 0.5$ . For  $x(\text{total}) = 1.5$  the dominant species appear to be cupric sites *unconnected* to the amine groups of the polymer.

The method of diamagnetic dilution clearly indicates the complexity of the ligation and the changes that occur with cation addition. All results appear to indicate that, as the amount of cations increases, the ions form a cluster that is separated from the polymer.

The results obtained in this study might explain the fact that  $T_g$  is not changed on cation addition: At low cation content the polymer is complexed to the cations, but the number of complexed chains is small and not reflected in the DSC measurements. As the cation content is higher, the chains are decomplexed, again giving the “normal” (nonionic)  $T_g$ . These results might also explain the increase in  $T_g$  after annealing at temperatures above  $T_g$ . The annealing process could break the cation clusters and disperse them in the ionomer matrix, thus forcing the contact of the chain ends with the cations and leading to a higher  $T_g$ .

The conclusions deduced from this study can be examined in view of the recent polemic on the effect of ions on the chain dimensions.<sup>31</sup> The chain dimensions in carboxy-terminated telechelic polystyrene neutralized by  $\text{Na}^+$  were found to be identical to those of the ester,<sup>15</sup> in agreement with some theoretical predictions<sup>32</sup> and in disagreement with others.<sup>33,34</sup> The results we presented suggest that at high cation content the polymer chains are expected to be relatively unaffected by the presence of the ions. The cations are organized in domains that act as *fillers* but do not modify the properties of the chains. It appears that the two systems have a similar behavior.

## Conclusions

ESR spectra of  $\text{Cu}^{2+}$  complexes in amine-terminated telechelic polybutadiene were measured, in order to obtain local information on the bonding in the cupric site. The increase in the line widths with cation content indicates the process of cation clustering. The intercation distances deduced from the broadening of the ESR lines are much shorter than those calculated by assuming of a homogeneous cation distribution and approach the Cu–Cu distance of 5.457 Å in  $\text{CuCl}_2 \cdot 2\text{H}_2\text{O}$  at a high content of the cation.

Diamagnetic dilution by  $\text{Zn}^{2+}$  allows observation of the details of polymer complexation with high resolution, even at a combined ( $\text{Cu}^{2+}$  and  $\text{Zn}^{2+}$ ) cation content 6 times higher than the theoretical amount needed for full complexation. The results obtained in this study indicate that the cation site is very sensitive to the total cation content. At a low degree of complexation  $\text{Cu}^{2+}$  is connected to the polymer through four  $^{14}\text{N}$  ligands. The number of nitrogen ligands decreases as the amount of cation increases. For a combined cation content 3 times higher than that needed for full complexation, the cations appear to form ionic domains isolated from, and unconnected to, the polymer chains.

The results obtained describe the complexity of the polymer bonding to the cation and indicate explicitly the various cation sites. The break in the polymer bonding to the cation at high cation content and the existence of the isolated ionic domains explain two effects discussed in the literature, the fact that both the  $T_g$  and the chain dimensions are not affected by the presence of the cations.

**Acknowledgment.** This research was supported by the donors of the Petroleum Research Fund, administered by the American Chemical Society, and by National Science Foundation Grant DMR-8718947 (Polymers Program). S.S. is grateful to the American Association of University Women (AAUW) for the 1991/1992 Founders' Fellowship. We thank David R. Egan of B.F. Goodrich for the gift of the Hycar ionomers.

## References and Notes

- (1) *Ion Containing Polymers*; Eisenberg, A., King, M., Eds.; Academic Press: New York, 1977.
- (2) *Perfluorinated Ionomer Membranes*; Eisenberg, A., Yeager, H. L., Eds.; ACS Symposium Series 180; American Chemical Society: Washington, DC, 1982.
- (3) *Structure and Properties of Ionomers*; Pineri, M., Eisenberg, A., Eds.; NATO Advanced Study Institute Series; Reidel: Dordrecht, The Netherlands, 1987.
- (4) Boyle, N. G.; Coey, J. M. D.; Meagher, A., McBrierty, V. J.; Nakano, Y.; MacKnight, W. J. *Macromolecules* **1984**, *17*, 1331.
- (5) Pineri, M.; Meyer, C.; Levelut, A. M.; Lambert, M. J. *Polym. Sci., Polym. Phys. Ed.* **1974**, *12*, 115.
- (6) Yamauchi, J.; Yano, S. *Makromol. Chem.* **1978**, *179*, 2799.
- (7) Toriumi, H.; Weiss, R. A.; Frank, H. A. *Macromolecules* **1984**, *17*, 2104.
- (8) Alonso-Amigo, M. G.; Schlick, S. *J. Phys. Chem.* **1989**, *93*, 7526.
- (9) Bednarek, J.; Schlick, S. *Langmuir* **1992**, *8*, 249.
- (10) Schlick, S.; Gebel, G.; Pineri, M.; Volino, F. *Macromolecules* **1991**, *24*, 3517.
- (11) *Telechelic Polymers: Synthesis and Applications*; Goethals, E., Ed.; CRC Press: Boca Raton, FL, 1989.
- (12) Williams, C. E.; Russell, T. P.; Jérôme, R.; Horrion, J. *Macromolecules* **1986**, *19*, 2877.
- (13) Horrion, J.; Jérôme, R.; Teyssié, Ph.; Marco, C.; Williams, C. E. *Polymer* **1988**, *29*, 1203.
- (14) Charlier, P.; Jérôme, R.; Teyssié, Ph.; Utracki, L. A. *Macromolecules* **1990**, *23*, 3313.
- (15) Register, R. A.; Copper, S. L.; Thiyagarajan, P.; Chakrapani, S.; Jérôme, R. *Macromolecules* **1990**, *23*, 2978.
- (16) Galland, D.; Belakhovsky, M.; Medrignac, F.; Pineri, M.; Vlaic, G.; Jérôme, R. *Polymer* **1986**, *27*, 883.
- (17) Yano, S.; Tadano, K.; Jérôme, R. *Macromolecules* **1991**, *24*, 6439.
- (18) McBrierty, V. J.; Smyth, G.; Douglass, D. C. In *Structure and Properties of Ionomers*; Pineri, M., Eisenberg, A., Eds.; NATO Advanced Study Institute Series; Reidel: Dordrecht, The Netherlands, 1987; p 149.
- (19) Alonso-Amigo, M. G.; Schlick, S. *Macromolecules* **1989**, *22*, 2628.
- (20) Schlick, S.; Alonso-Amigo, M. G. *Macromolecules* **1989**, *22*, 2634.
- (21) Bednarek, J.; Schlick, S. *J. Am. Chem. Soc.* **1990**, *112*, 5019.
- (22) Bednarek, J.; Schlick, S. *J. Am. Chem. Soc.* **1991**, *113*, 3303.
- (23) Maiti, B.; Schlick, S. *Chem. Mater.* **1992**, *4*, 458.
- (24) Bunce, N. J.; Sondheimer, S. J.; Fyfe, C. A. *Macromolecules* **1986**, *19*, 333.
- (25) Riew, C. K. In Proceedings of the Rubber Division. American Chemical Society Meeting, Detroit, MI, 1980.
- (26) Peisach, J.; Blumberg, W. E. *Arch. Biochem. Biophys.* **1974**, *165*, 691.
- (27) Hathaway, B. J.; Billing, D. E. *Coord. Chem. Rev.* **1970**, *5*, 143.
- (28) McGarvey, B. R. In *Transition Metal Chemistry*; Carlin, R. L., Ed.; Marcel Dekker: New York, 1966; Vol. 3.
- (29) Abragam, A. *Principles of Nuclear Magnetism*; Oxford University Press: Oxford, U.K., 1983; Chapter IV, p 106.
- (30) Wyckoff, R. W. G. *Crystal Structures*; Interscience Publishers: New York, 1960; Chapters IV and X.
- (31) Feng, D.; Wilkes, G. L. *Macromolecules* **1991**, *24*, 6789.
- (32) Squires, E.; Painter, P.; Howe, S. *Macromolecules* **1987**, *20*, 1740.
- (33) Forsman, W. C.; MacKnight, W. J.; Higgins, J. S. *Macromolecules* **1984**, *17*, 490.
- (34) Dreifus, B. *Macromolecules* **1985**, *18*, 284.

**Registry No.** Zn, 7440-66-6.